91602
new 82-10

ontario hydro
research division

EXTENSIONS TO A COMPUTER PROGRAM FOR PERFORMING ENGINEERING APPROACH ELASTIC-PLASTIC FRACTURE MECHANICS FLAW EVALUATIONS

Report No. 88-290-K

D.A. Scarth
Nondestructive and Fracture Evaluation Section
Metallurgical Research Department

ABSTRACT

A computer program was previously written to perform Elastic-Plastic Fracture Mechanics (EPFM) flaw evaluations based on the J-Integral/Tearing Modulus Engineering Approach. The only flaw model in the original version of the program was a circular cylinder containing a 360° circumferential edge crack under tension. This version was modified to include a two-dimensional "infinitely long" axial flaw model, and a three-dimensional semi-elliptical axial flaw model. Membrane and bending secondary stresses have also been included in all the flaw models. Given in this report is an outline of the basic theory, the flaw evaluation procedures which are in the program, validation cases, and a user input description for the program.

job	file	date	report no.
83-272-452	826.241	January 16, 1989	88-290-K

91602
new 82-10

ontario hydro
research division

EXECUTIVE SUMMARY

EXTENSIONS TO A COMPUTER PROGRAM FOR PERFORMING ENGINEERING APPROACH ELASTIC-PLASTIC FRACTURE MECHANICS FLAW EVALUATIONS

Report No. 88-290-K

D.A. Scarth
Nondestructive and Fracture Evaluation Section
Metallurgical Research Department

A computer program was previously written to perform Elastic-Plastic Fracture Mechanics (EPFM) flaw evaluations based on the J-Integral/Tearing Modulus Engineering Approach. The program, named EPFLAW, provides an efficient means to solve the nonlinear equations involved in EPFM flaw evaluations.

The only flaw model in the original version of EPFLAW was a circular cylinder containing a 360° circumferential edge crack under tension. This Version 1.0 of EPFLAW was modified to Version 2.0 to include a two-dimensional "infinitely long" axial flaw model, and a three-dimensional semi-elliptical axial flaw model. Membrane and bending secondary stresses have also been included in all the flaw models. Given in this report is an outline of the basic theory of the J-Integral/Tearing Modulus Engineering Approach used in the computer program. Also given are the flaw evaluation procedures which are in the program as well as validation cases. A user input description for the program is included.

The program is designed to allow the user to perform automated scoping calculations for a flaw. References are also made to other EPFM flaw evaluation procedures which are available to Ontario Hydro.

job	file	date	report no.
83-272-452	826.241	January 16, 1989	88-290-K

TABLE OF CONTENTS

		Page
1.0	INTRODUCTION	1
2.0	CONCLUSIONS AND RECOMMENDATIONS	2
3.0	BACKGROUND	3
3.1	Basic Theory of Ductile Tearing Instability	3
3.2	The Engineering Approach – J-Integral Estimation Formulae	4
3.3	J-Controlled Crack Growth	5
3.4	Curve Fitting Material Stress-Strain and J-Integral Resistance Curves	6
4.0	DESCRIPTION OF MODELS	8
4.1	Flaw Model 1 – Circular Cylinder Containing an Inner 360° Circumferential Edge Crack Under Tension	8
4.2	Flaw Model 2 – Circular Cylinder Containing an Infinitely Axial Crack Under Internal Pressure	9
4.3	Flaw Model 3 – Circular Cylinder Containing a Semi-Elliptical Axial Crack Under Internal Pressure	10
4.4	J-Integral Resistance Curve Model 1 – Power Law	11
5.0	PROCEDURES	22
5.1	Procedure 1 – Generate J-Integral and Tearing Modulus	22
5.2	Procedure 2 – Follow a J-R Curve	22
5.3	Procedure 3 – Finding Limiting Initial Flaw Depth	23
6.0	VALIDATION	23
REFERENCES		25
APPENDIX A:	Formulation of the Fully-Plastic h_1 Function for Semi-Elliptical Axial Flaws	46
APPENDIX B:	Input Description	49
DISTRIBUTION		last page

LIST OF TABLES

Table 4–1 Validity Limits for Flaw Models

Table 4–2 F Calibration Function for a Circumferentially Cracked Cylinder in Tension (from /3/)

Table 4–3 h_1 Calibration Function for a Circumferentially Cracked Cylinder in Tension with t/R_i = 0.20 (from /3/)

Table 4–4 h_1 Calibration Function for a Circumferentially Cracked Cylinder in Tension with t/R_i = 0.10 (from /3/)

Table 4–5 h_1 Calibration Function for a Circumferentially Cracked Cylinder in Tension with t/R_i = 0.05 (from /3/)

Table 4–6 F Calibration Function for an Axially Cracked Cylinder Under Internal Pressure (from /3/)

Table 4–7 Elastic Geometry Correction Factors for an Axially Cracked Cylinder Subject to Membrane and Through-Wall Bending Hoop Stress (from /12/)

Table 4–8 h_1 Calibration Function for an Axially Cracked Cylinder Under Internal Pressure with t/R_i = 0.20 (from /3/)

Table 4–9 h_1 Calibration Function for an Axially Cracked Cylinder Under Internal Pressure with t/R_i = 0.10 (from /3/)

Table 4–10 h_1 Calibration Function for an Axially Cracked Cylinder Under Internal Pressure with t/R_i = 0.05 (from /3/)

Table 4–11 G_i Elastic Calibration Functions for a Cylinder Containing a Semi-Elliptical Axial Flaw Under Internal Pressure (from /3/)

Table 4–12 h_1 Calibration Function for a Cylinder Containing a Semi-Elliptical Axial Crack (a/c = 0.333) Under Internal Pressure with t/R_i = 0.10

Table 6–1 Dimensions of Models Used in the Validation Cases

Table 6–2 Material properties for Validation Cases

Table 6–3 Applied Loads Used in the Validation of Procedure 1

Table 6–4 Results from Validation of Procedure 1

Table 6–5 Applied Loads Used in the Validation of Procedure 2

Table 6–6 Inputted Controlling Parameters for Validation of Procedure 2 Using Model 1

Table 6-7 Results of Validation of Procedure 2 Using Model 1

Table 6-8 Inputted Controlling Parameters for Validation of Procedure 2 Using Model 2

Table 6-9 Results of Validation of Procedure 2 Using Model 2

Table 6-10 Inputted Controlling Parameters for Validation of Procedure 2 Using Model 3

Table 6-11 Results of Validation of Procedure 2 Using Model 3

Table 6-12 Applied Loads Used in the Validation of Procedure 3

Table 6-13 Inputted Controlling Parameters for Validation of Procedure 3 using Model 1

Table 6-14 Results of Validation of Procedure 3 Using Model 1

Table 6-15 Inputted Controlling Parameters for Validation of Procedure 3 Using Model 2

Table 6-16 Results of Validation of Procedure 3 Using Model 2

Table 6-17 Inputted Controlling Parameters for Validation of Procedure 3 Using Model 3

Table 6-18 Results of Validation of Procedure 3 Using Model 3

LIST OF FIGURES

Figure 3-1 Material J-integral Resistance Curve

Figure 4-1 Cylinder Containing an Inner 360° Circumferential Edge Crack Under Tension

Figure 4-2 Cylinder Containing an Infinitely Long Axial Crack Under Internal Pressure

Figure 4-3 Cylinder Containing a Semi-Elliptical Axial Crack Under Internal Pressure

In Appendix A

Figure A-1 Variation of h_1 Function With a/t for Semi-Elliptical Axial Crack, with $a/c = 1/3$, $t/R_i = 0.10$ and $n = 8.6$

ontario hydro
research division

To

Mr. B. Montford
Manager
Chemistry and Metallurgy
Central Nuclear Services
Technical and Training Services
A7H9

EXTENSIONS TO A COMPUTER PROGRAM FOR PERFORMING ENGINEERING APPROACH ELASTIC-PLASTIC FRACTURE MECHANICS FLAW EVALUATIONS

1.0 INTRODUCTION

Linear-Elastic Fracture Mechanics (LEFM) is based on the postulate that unstable fracture of a cracked structure will occur once crack extension is initiated. Elastic-Plastic Fracture Mechanics (EPFM) differs from LEFM in that after initiation some stable crack extension is modelled. This leads to more accurate estimates of the real safety margins for a flawed structure. The application of EPFM has been simplified by the development of the J-Integral/Tearing Modulus Engineering Approach/3,4/. In this approach the elastic-plastic J-integral/5/ is used as a fracture criterion. However, one must still solve a set of nonlinear equations either graphically or by using a numerical technique.

To facilitate efficient solutions of these equations for the purposes of performing EPFM flaw evaluations, a computer program, EPFLAW - Version 1.0, was written/6/. The solution procedures built into the program will minimize the efforts involved in performing an EPFM flaw evaluation. Version 2.0 of EPFLAW has been completed. Version 2.0 now contains axial flaw models in addition to the circumferential flaw model in Version 1.0. A user's input manual is given in Appendix B of this report. The program is written in structured FORTRAN 77 existing on the VAX/VMS operating system supplied by Digital Equipment Corp.

Prior to performing an EPFM flaw evaluation, the user must have a good understanding of the structural behaviour of the flawed component, to ensure that the loading and deformation of the component is consistent with that of the particular estimation-scheme flaw model.

This work was performed with the support of the Chemistry and Metallurgy Department of Central Nuclear Services.

2.0 CONCLUSIONS AND RECOMMENDATIONS

CONCLUSIONS

a) Extensions have been added to the computer program EPFLAW, which is used to perform elastic-plastic fracture mechanics evaluations of flaws. The program is based on the J-Integral/Tearing Modulus Engineering Approach.

b) The program now includes flaw models of a circular cylinder containing a 360° circumferential edge crack under tension, a circular cylinder containing an inner "infinitely long" axial edge crack under internal pressure, and a circular cylinder containing an inner semi-elliptical axial crack under internal pressure. Secondary membrane and pure through-wall bending stresses are included in all of the flaw models.

c) Validation of all flaw models and evaluation procedures in the computer program has been completed.

d) The computer program is modular in structure and other flaw models can be implemented expediently on an as-needed basis.

RECOMMENDATIONS

a) Prior to performing an EPFM flaw evaluation, the user must have a good understanding of the structural behaviour of the flawed component, to ensure that the loading and deformation of the component is consistent with that of the particular estimation-scheme flaw model.

b) The procedures in this computer program are designed to support automated scoping calculations in which various combinations of safety margins on load and on flaw depth are determined.

c) When curve fitting the material stress-strain curve, the conservative approach is to fit a lower-bound curve. When evaluating a flaw in a weldment, the conservative approach is to use the lower of the base metal and weld metal stress strain curves (usually the base metal), and the lower of the base metal and weld metal J-integral resistance curves (usually the weld metal).

d) When using this program to arrive at conclusions regarding the disposition of a flaw, the final margins output by the program should be checked against an alternate calculation procedure.

e) In addition to this computer program, other flaw evaluation procedures currently available to Ontario Hydro should be utilized when possible. These include the flaw evaluation procedures for ferritic piping being incorporated into Section XI of the ASME Boiler and Pressure Vessel Code/1/, as well as the commercial computer program pc-FAD/2/ (purchased from Babcock and Wilcox).

3.0 BACKGROUND

3.1 Basic Theory of Ductile Tearing Instability

The elastic-plastic J-integral/5/ is used as a fracture criterion. The first condition is a statement of equilibrium

$$J_R(\Delta a) = J_{ep}(a,P,\sigma^s) \tag{3.1}$$

where $J_R(\Delta a)$ is the material's J-integral resistance at a crack extension of Δa, and $J_{ep}(a,P,\sigma^s)$ is the applied elastic-plastic J-integral (crack-driving force) for a crack depth a, applied primary load P (eg. internal pressure) and secondary stress σ^s (eg. thermal stress). The J-Integral Resistance Curve (J-R Curve) is obtained experimentally from laboratory specimens and is considered to be a material property under certain restrictions. One J-integral resistance curve is illustrated in Figure 3-1.

As the applied load increases, the applied J-integral increases and the material's J-integral resistance also increases. Further crack extension occurs simultaneously. The point defined by equation (3.1) moves up along the J-R curve. At some point the rate of increase in the applied J-integral will exceed the rate of increase in the material's resistance J-integral and the crack will become unstable. This assumes load-controlled conditions/3/ which typically characterize a component loaded by internal pressure. For crack extension to remain stable the following equation must be satisfied:

$$\frac{dJ_R(\Delta a)}{da} \geq \left(\frac{\partial J_{ep}(a,P,\sigma^s)}{\partial a}\right)_P \tag{3.2}$$

where $(\quad)_p$ denotes partial differentiation with the load P held constant. The material resistance tearing modulus is defined as

$$T_R = \frac{E}{\sigma_f^2}\frac{dJ_R(\Delta a)}{da} \tag{3.3}$$

where E is Young's modulus and σ_f is the flow stress. The applied tearing modulus for load-controlled conditions is

$$T_J = \frac{E}{\sigma_f^2}\left(\frac{\partial J_{ep}(a,P,\sigma^s)}{\partial a}\right)_P . \tag{3.4}$$

Equation (3.2) can be restated as

$$T_R \geq T_J \tag{3.5}$$

for stability. Unstable ductile tearing will occur once the applied load and crack extension have reached the point that T_J exceeds T_R. The combined J-integral/tearing modulus analysis is known as the J/T Approach. Further discussion can be found in/3,4,7/.

3.2 The Engineering Approach – J-Integral Estimation Formulae

The so-called "Engineering Approach" to elastic-plastic fracture mechanics is employed in which the elastic-plastic J-integral is calculated by using relatively simple estimation formulae. In these formulae the J-integral is scaled on load. Implicit in using this approach is the assumption that the material is subjected to proportional loading such that the use of deformation plasticity theory/8/ is valid. The engineering approach is documented in references/3,4/.

The applied elastic-plastic J-integral is estimated by a summation of the elastic and fully-plastic portions.

$$J_{ep}(a,P,\sigma^s) = J_e(a_e,P,\sigma^s) + J_p(a,P) \tag{3.6}$$

Here $J_e(a_e,P,\sigma^s)$ is the elastic J-integral for small-scale yielding given by

$$J_e(a_e,P,\sigma^s) = \frac{K_I(a_e,P,\sigma^s)^2}{E'} \tag{3.7}$$

where $K_I(a_e,P,\sigma^s)$ is the stress intensity factor for small-scale yielding determined from well-documented formulae. A general expression for K_I for a given flaw depth a is

$$K_I = \left(\frac{\pi a}{Q}\right)^{1/2} [P\ F_p(a/t) + \sigma_m{}^s\ F_m(a/t) + \sigma_b{}^s\ F_b(a/t)] \tag{3.8}$$

where Q is the flaw shape parameter given by

$$Q = 1 + 1.464\ (a/c)^{1.65}, \tag{3.9}$$

t is the wall thickness and c is the half-length of the flaw.

The $F_p(a/t)$ is the geometry correction factor for the primary load P, $F_m(a/t)$ is the geometry correction factor for the secondary membrane stress $\sigma_m{}^s$, and $F_b(a/t)$ is the geometry correction factor for the secondary pure through-wall bending stress $\sigma_b{}^s$. The term E' is given by

$$\begin{aligned} E' &= E/(1-\nu^2) \text{ for plane strain,} \\ E' &= E \text{ for plane stress} \end{aligned} \tag{3.10}$$

where ν is Poisson's ratio.

The effective flaw depth a_e contains a modified Irwin's plastic zone correction and is given by

$$a_e = a + \phi r_y \quad . \tag{3.11}$$

Here ϕ is an interpolation function,

$$\phi = 1/(1 + (P/P_o)^2) \tag{3.12}$$

where P_o is the reference limit load. Also,

$$r_y = \frac{1}{\beta\pi}\left[\frac{n-1}{n+1}\right]\left(\frac{K_I(a,P,\sigma^s)}{\sigma_o}\right)^2 \tag{3.13}$$

where
$$\beta = 2 \text{ for plane stress,}$$
$$\beta = 6 \text{ for plane strain,} \tag{3.14}$$

$K_I(a,P,\sigma^s)$ is the linear-elastic stress intensity factor based on the flaw depth a, and σ_o is the yield stress. The constant n is the strain hardening exponent determined by a fit of the material's uniaxial true stress/true strain curve to the Ramberg-Osgood idealized true stress/true strain equation/3/

$$\frac{\varepsilon}{\varepsilon_o} = \frac{\sigma}{\sigma_o} + \alpha\left(\frac{\sigma}{\sigma_o}\right)^n \tag{3.15}$$

where ε is true strain, ε_o is the yield strain ($= \sigma_o/E$), σ is the true stress and α is a material constant.

The fully-plastic portion of the J-integral is estimated for cylindrical geometries by using

$$J_p(a,P) = \alpha\,\sigma_o\,\varepsilon_o\,a\,g_1(a)\,h_1(a/c,\ a/t,\ t/R_i,n)\left(\frac{P}{P_o(a)}\right)^{n+1} \tag{3.16}$$

where α is given in equation (3.15), $g_1(a)$ is a geometry dependent function, R_i is the inside radius of the cylinder and h_1 is a nondimensional function which is usually calibrated to elastic-plastic finite-element results. Following /9/, the fully-plastic portion of the J-integral is dependent on the primary load but not on secondary stress. This is due to the fact that secondary stresses are self-equilibrating.

The applied tearing modulus is obtained by analytical differentiation of equations (3.7) and (3.16).

3.3 J-Controlled Crack Growth

Three criteria have been identified in /3/ to check that the crack extension process is in fact controlled by the magnitude of the J-integral. These criteria should be applied to determine the limit of validity of data from laboratory specimens, and the limit of validity for modelling crack growth in a component.

One requirement is to ensure that the crack-tip plastic zone is fully contained by the remaining ligament, b. This is written as

$$\Delta a < 0.06\ b, \tag{3.17}$$

where Δa is the crack extension. For the case of obtaining the material's resistance curve from a compact tension specimen, it is recommended in /10/ that

$$\Delta a < 0.10\ b \quad . \tag{3.18}$$

A second requirement is that the change in the magnitude in the deformation field surrounding the crack tip be governed by a change in the J-integral as opposed to a change in the crack depth. A parameter ω is defined in /3/ as

$$\omega = \frac{b}{J_{Ic}} \frac{dJ_R}{da} \tag{3.19}$$

where J_{Ic} is the material's J-integral value at crack initiation. For components subjected primarily to bending it is recommended in /3/ that $\omega > 10$, while for components subjected primarily to tension, $\omega > 80$. In the computer program the actual value of J will be used in place of J_{Ic} in equation (3.19).

A third criterion is that the crack-tip opening displacement be much smaller than the remaining ligament. A parameter ρ is defined as

$$\rho = \frac{b\ \sigma_o}{J_R} \quad . \tag{3.20}$$

In /3/ it is recommended that for components subjected primarily to bending, $\rho > 25$, and for components subjected primarily to tension, $\rho > 200$.

All three criteria are employed in the computer program. The criteria are not rigorous, and may be exceeded provided the problem is well understood and exceeding the limits can be demonstrated to be conservative.

3.4 Curve Fitting Material Stress-Strain and J-Integral Resistance Curves

When choosing a yield stress the conservative approach is to choose a lower-bound yield stress. When curve fitting the material stress-strain curve, the conservative approach is to fit a lower-bound curve.

When evaluating a flaw in a weldment, the conservative approach is to use the lower of the base metal and weld metal stress-strain curves (usually the base metal), and the lower of the base metal and weld metal J-integral resistance curves (usually the weld metal).

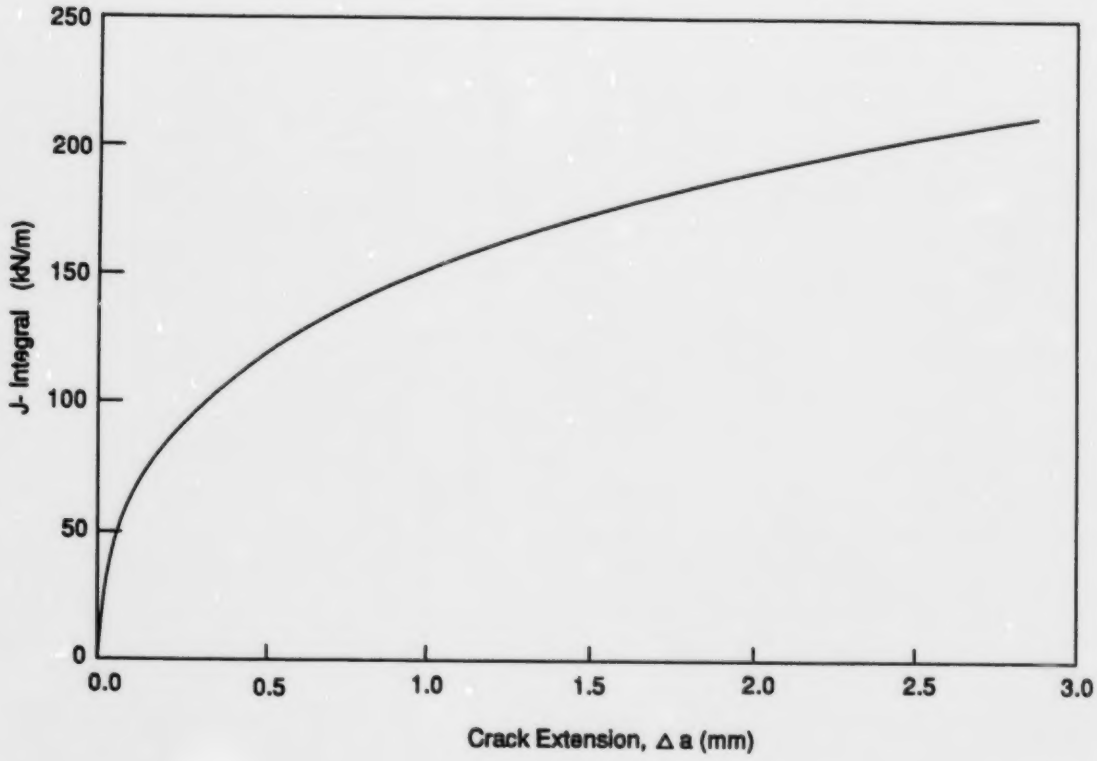

FIGURE 3-1

MATERIAL J-INTEGRAL RESISTANCE CURVE

4.0 DESCRIPTION OF MODELS

4.1 Flaw Model 1 – Circular Cylinder Containing an Inner 360° Circumferential Edge Crack Under Tension

This model is a circular cylinder with inner radius R_i, outer radius R_o, wall thickness t and infinite length. The cylinder contains an inner 360° circumferential edge crack of depth a. The cylinder is under a remote tensile primary stress P, a secondary membrane stress σ_m^s and a pure through-wall bending secondary stress σ_b^s. The model is illustrated in Figure 4–1. The functions included in Section 3.2 which are specific to the model are given below. The range of validity of the model in terms of a/t, t/R_i and n are given in Table 4–1.

Crack-Tip Stress Intensity Factor

The geometry correction factor for the primary membrane stress P is

$$F_p(a/t) = F(a/t,\ t/R_i), \tag{4.1}$$

where $F(a/t,\ t/R_i)$ is a calibrated function taken from reference /3/ and given in Table 4–2 of this report.

The geometry correction factor for the secondary membrane stress σ_m^s is the same as that for the primary membrane stress.

$$F_m(a/t) = F(a/t,\ t/R_i) \text{ from /3/.} \tag{4.2}$$

The geometry correction factor for the secondary pure through-wall bending stress σ_b^s is taken from the solution for an edge-cracked plate under pure bending/11/.

$$F_b(a/t) = 1.122 - 1/40(a/t) + 7.33(a/t)^2 - 13.08(a/t)^3 + 15.0(a/t)^4 \tag{4.3}$$

The last term contains the multiplier "15.0" rather than the "14.0" given in the polynomial expression in /11/. This term was modified to produce better agreement with more exact solutions given in /11/ when a/t approaches 0.75.

Fully-Plastic J-Integral

The fully-plastic solution was taken from the EPRI handbook/3/. The reference limit load is written as

$$P_o = \frac{2}{\sqrt{3}} \pi \sigma_o (R_o^2 - R_c^2) \tag{4.4}$$

where

$$R_c = R_i + a \quad . \tag{4.5}$$

Plane-strain conditions exist at the crack tip such that $E' = E/(1 - \nu^2)$ and $\beta = 6$. The function g_1 is given by

$$g_1 = 1 - a/t \tag{4.6}$$

The function $h_1(a/t, t/R_i, n)$ is given in tabular format in Tables 4-3 to 4-5.

4.2 Flaw Model 2 - Circular Cylinder Containing an Infinitely Long Axial Crack Under Internal Pressure

This model is a circular cylinder with inner radius R_i, outer radius R_o, wall thickness t, and is of infinite length. The cylinder contains an inner edge crack of depth a and of infinite length. The cylinder is subjected to an internal pressure p, a secondary membrane stress σ_m^s, and a secondary pure through-wall bending stress σ_b^s. The model is illustrated in Figure 4-2. The functions included in Section 3.2 which are specific to the model are given below. The range of validity of the model in terms of a/t, t/R_i and n are given in Table 4-1.

Crack-Tip Stress Intensity Factor

The geometry correction factor for the internal pressure p (primary load) is

$$F_p(a/t) = \frac{2R_o^2}{(R_o^2 - R_i^2)} F(a/t, R_i/R_o) \tag{4.7}$$

where $F(a/t, R_i/R_o)$ is a calibrated tabular function taken from the EPRI handbook/3/ and given in Table 4-6 of this report.

The geometry correction factor for the secondary membrane stress σ_m^s is

$$F_m(a/t) = F_1(a/t) \tag{4.8}$$

where $F_1(a/t)$ was taken from Buchalet and Bamford/12/ and is given in Table 4-7. The geometry correction factor for the secondary pure through-wall bending stress σ_b^s is given by

$$F_b(a/t) = F_1(a/t) - (4/\pi)(a/t)\, F_2(a/t) \tag{4.9}$$

where $F_2(a/t)$ was also taken from /12/ and is given in Table 4-7.

Fully-Plastic J-Integral

The fully-plastic solution was taken from the EPRI handbook/3/. The reference limit pressure is

$$p_o = \frac{2\,(t-a)\,\sigma_o}{\sqrt{3}\,(R_i + a)} \tag{4.10}$$

Plane-strain conditions exist at the crack tip such that $E' = E/(1 - \nu^2)$ and $\beta = 6$. The function g_1 is given by

$$g_1 = 1 - a/t \tag{4.11}$$

The function $h_1(a/t, t/R_i, n)$ is given in tabular format in Tables 4-8 to 4-10.

4.3 Flaw Model 3 – Circular Cylinder Containing a Semi-Elliptical Axial Crack Under Internal Pressure

This model is a circular cylinder with inner radius R_i, outer radius R_o, wall thickness t, and is of infinite length. The cylinder contains an inner semi-elliptical axial crack of depth a and half-length c. The cylinder is subjected to an internal pressure p, a secondary membrane stress σ_m^s, and a secondary pure through-wall bending stress σ_b^s. The model is illustrated in Figure 4-3. The functions included in Section 3.2 which are specific to the model are given below. The range of validity of the model in terms of a/t, a/c, t/R_i and n are given in Table 4-1. Two sets of validity limits are given: one set for the full elastic-plastic case; and one set for the case of elastic conditions with small-scale yielding (plastic-zone correction). The full elastic-plastic case is much more restrictive, limited to a/c = 1/3 and t/R_i = 0.10.

Crack-Tip Stress Intensity Factor

The geometry correction factor for the internal pressure p (primary load) is

$$F_p(a/t) = \frac{R_o^2}{R_o^2 - R_i^2} \left[2\,G_o - 2(a/R_i)\,G_1 + 3(a/R_i)^2\,G_2 - 4(a/R_i)^3\,G_3\right] \qquad (4.12)$$

where the calibrated functions G_i are given in tabular form by Raju and Newman/13/ and are a function of a/t, a/c, t/R_i and the location along the crack front. The values of G_i for the deepest point of penetration are given in Table 4-11. The lowest a/t for which the G_i functions are given in /13/ is a/t = 0.20. This will result in a slight over-estimate of K_I by an amount not exceeding 5% when used for a/t = 0.125.

The geometry correction factor for the secondary membrane stress σ_m^s is given by

$$F_m(a/t) = G_o \qquad (4.13)$$

where G_o is given in /13/.

The geometry correction factor for the secondary pure through-wall bending stress σ_b^s is

$$F_b(a/t) = G_o - 2(a/t)\,G_1 \qquad (4.14)$$

Fully-Plastic J-Integral

The solution was based on results given by Wilkening et al/14/, Bloom/15/ and some in-house finite-element calculations. The reference limit load is taken from /15/

$$P_o = (2/\sqrt{3})(t/R_i)\ \sigma_o \left(\frac{1 - a^*/t}{1 + (t/R_i)(a^*/t)} \right) \qquad (4.15)$$

where

$$a^* = a \left(\frac{1 - 1/(1+2(c/t)^2)^{0.5}}{1 - (a/t)/(1 + 2(c/t)^2)^{0.5}} \right) \qquad (4.16)$$

Plane-strain conditions exist at the crack tip such the $E' = E/(1 - \nu^2)$ and $\beta = 6$.

The function g_1 is given by

$$g_1 = 1 - a/t \qquad (4.17)$$

The function $h_1(a/t,\ a/c,\ t/R_i,\ n)$ is given in Table 4-12. Details on the formulation of h_1 are given in Appendix A of this report.

4.4 J-Integral Resistance Curve Model 1 - Power Law

The material's J-Integral Resistance Curve (J-R Curve) is represented by a power-law equation.

$$J_R = C_1\ (\Delta a)^{C_2} \qquad (4.18)$$

The material's resistance tearing modulus is given by

$$T_R = \frac{E}{\sigma_f^2}\ C_1\ C_2\ (\Delta a)^{C_2 - 1} \qquad (4.19)$$

TABLE 4-1

Validity Limits for Flaw Models

Flaw Model	a/t		a/c		t/R_i		n	
	Min	Max	Min	Max	Min	Max	Min	Max
Model 1 360° Circumferential Flaw	0.125	0.750	0.0	0.0	0.05	0.20	1.0	10.0
Model 2 Infinitely Long Axial Flaw	0.125	0.750	0.0	0.0	0.05	0.20	1.0	10.0
Model 3 Semi-Elliptical Axial Flaw	0.125	0.750	0.333	0.333	0.10	0.10	7.0	10.0
Model 3 for Elastic Case with Small-Scale Yielding	0.125	0.750	0.200	1.000	0.10	0.25	-	-

TABLE 4-2

F Calibration Function for a Circumferentially Cracked Cylinder in Tension (from /3/)

	a/t			
t/R_i	0.125	0.250	0.500	0.750
0.20	1.16	1.26	1.61	2.15
0.10	1.19	1.32	1.82	2.49
0.05	1.22	1.36	2.03	2.89

TABLE 4-3

h_1 Calibration Function for a Circumferentially Cracked Cylinder in Tension With t/R_i = 0.20 (from /3/)

	n					
a/t	1	2	3	5	7	10
0.125	3.78	5.00	5.94	7.54	8.99	11.1
0.250	3.88	4.95	5.64	6.49	6.94	7.22
0.500	4.40	4.78	4.59	3.79	3.07	2.34
0.750	4.12	3.03	2.23	1.546	1.30	1.11

TABLE 4-4

h_1 Calibration Function for a Circumferentially Cracked Cylinder in Tension With $t/R_i = 0.10$ (from /3/)

	n					
a/t	1	2	3	5	7	10
0.125	4.00	5.13	6.09	7.69	9.09	11.1
0.250	4.17	5.35	6.09	6.93	7.30	7.41
0.500	5.40	5.90	5.63	4.51	3.49	2.47
0.750	5.18	3.78	2.57	1.59	1.31	1.10

TABLE 4-5

h_1 Calibration Function for a Circumferentially Cracked Cylinder in Tension With $t/R_i = 0.05$ (from /3/)

	n					
a/t	1	2	3	5	7	10
0.125	4.04	5.23	6.22	7.82	9.19	11.1
0.250	4.38	5.68	6.45	7.29	7.62	7.65
0.500	6.55	7.17	6.89	5.46	4.13	2.77
0.750	6.64	4.87	3.08	1.68	1.30	1.07

TABLE 4-6

F Calibration Function for an Axially Cracked Cylinder Under Internal Pressure (from /3/)

	a/t			
t/R_i	0.125	0.250	0.500	0.750
0.20	1.19	1.38	2.10	3.30
0.10	1.20	1.44	2.36	4.23
0.05	1.20	1.45	2.51	5.25

TABLE 4-7

Elastic Geometry Correction Factors for an Axially Cracked Cylinder Subject to Membrane and Through-Wall Bending Hoop Stress (From /12/)

a/t	F_1	F_2
0.0	1.12	1.12
0.10	1.22	1.12
0.22	1.43	1.23
0.30	1.61	1.35
0.45	2.20	1.73
0.50	2.44	1.86
0.70	3.87	2.68
0.80	5.01	3.27

TABLE 4-8

h_1 Calibration Function for An Axially Cracked Cylinder Under Internal Pressure with $t/R_i = 0.20$ (from /3/)

	n					
a/t	1	2	3	5	7	10
0.125	6.32	7.93	9.32	11.5	13.12	14.94
0.250	7.00	8.34	9.03	9.59	9.71	9.45
0.500	9.79	10.37	9.07	5.61	3.52	2.11
0.750	11.0	5.54	2.84	1.24	0.83	0.493

TABLE 4-9

h_1 Calibration Function for An Axially Cracked Cylinder Under Internal Pressure with $t/R_i = 0.10$ (from /3/)

	n					
a/t	1	2	3	5	7	10
0.125	5.22	6.64	7.59	8.76	9.34	9.55
0.250	6.16	7.49	7.96	8.08	7.78	6.98
0.500	10.5	11.6	10.7	6.47	3.95	2.27
0.750	16.1	8.19	3.87	1.46	1.05	0.787

TABLE 4-10

h_1 Calibration Function for An Axially Cracked Cylinder Under Internal Pressure with $t/R_i = 0.05$ (from /3/)

	n					
a/t	1	2	3	5	7	10
0.125	4.50	5.79	6.62	7.65	8.07	7.75
0.250	5.57	6.91	7.37	7.47	7.21	6.53
0.500	10.8	12.8	12.8	8.16	4.88	2.62
0.750	23.1	13.1	5.87	1.90	1.23	0.883

TABLE 4-11

G_i Elastic Calibration Functions for a Cylinder Containing a Semi-Elliptical Axial Flaw Under Internal Pressure (from /13/)

Function	t/R_i	a/c								
		0.20			0.40			1.00		
		a/t			a/t			a/t		
		0.20	0.50	0.80	0.20	0.50	0.80	0.20	0.50	0.80
G_0	0.10	1.115	1.427	1.872	1.072	1.217	1.393	1.015	1.050	1.090
G_1	0.10	0.673	0.783	0.960	0.672	0.723	0.806	0.715	0.729	0.760
G_2	0.10	0.514	0.571	0.671	0.523	0.549	0.601	0.588	0.596	0.618
G_3	0.10	0.438	0.462	0.529	0.441	0.456	0.493	0.512	0.515	0.532
G_0	0.25	1.097	1.405	1.959	1.057	1.193	1.443	1.009	1.041	1.105
G_1	0.25	0.666	0.776	0.996	0.666	0.715	0.828	0.713	0.726	0.768
G_2	0.25	0.511	0.567	0.692	0.520	0.545	0.614	0.588	0.594	0.623
G_3	0.25	0.426	0.460	0.542	0.439	0.454	0.509	0.511	0.515	0.536

TABLE 4-12

h_1 Calibration Function for a Cylinder Containing a Semi-Elliptical Axial Crack (a/c = 0.333) Under Internal Pressure With t/R_i = 0.10

a/t	n		
	7	8.6	10
0.125	18.0	20.0	22.0
0.250	8.379	8.367	8.258
0.375	3.90	3.50	3.10
0.500	1.815	1.464	1.164
0.625	0.845	0.613	0.437
0.750	0.393	0.256	0.164

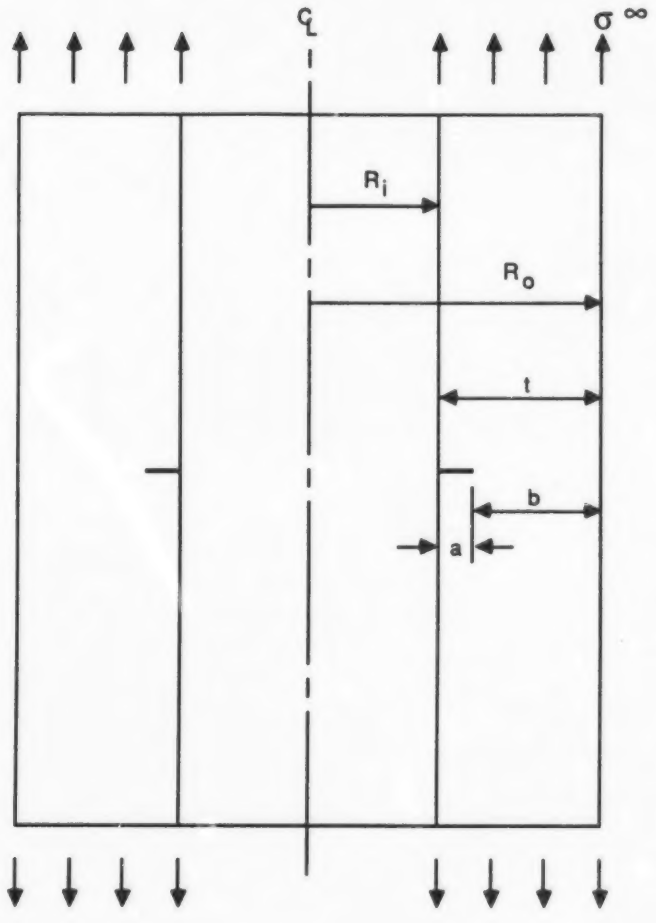

FIGURE 4-1
CYLINDER CONTAINING AN INNER 360°
CIRCUMFERENTIAL EDGE CRACK UNDER TENSION

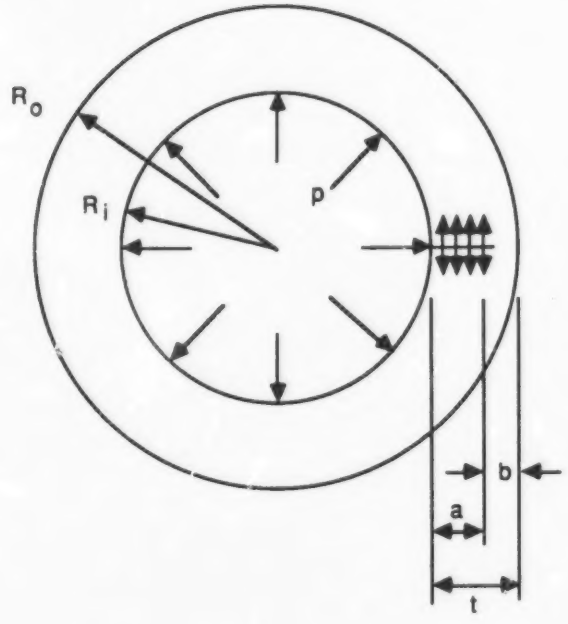

FIGURE 4-2
CYLINDER CONTAINING AN INFINITELY LONG AXIAL CRACK UNDER INTERNAL PRESSURE

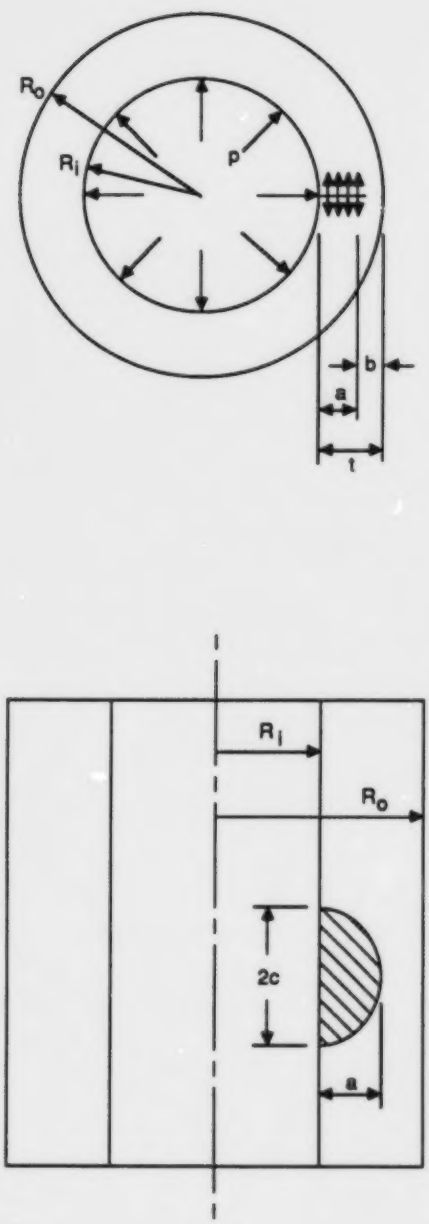

FIGURE 4-3
CYLINDER CONTAINING A SEMI-ELLIPTICAL AXIAL CRACK UNDER INTERNAL PRESSURE

5.0 PROCEDURES

There are three procedures in the computer program:

Procedure 1 – Generate the J-integral and tearing modulus.

Procedure 2 – From an initial flaw depth a_o, model ductile tearing by following a material J-R curve until some limit (eg. instability) is reached.

Procedure 3 – Repeat Procedure 2 for increasing values of initial flaw depth a_o until the safety margin on primary load is reduced to a specified value. This produces a limiting initial flaw depth.

An input description (user's manual) for each procedure is given in Appendix B.

5.1 Procedure 1 – Generate J-Integral and Tearing Modulus

The user inputs the model dimensions, material tensile properties, and various combinations of flaw size and loads. The elastic-plastic J-integral and tearing modulus are calculated and printed out for each combination.

5.2 Procedure 2 – Follow a J-R Curve

The user inputs the model dimensions, flaw size, material's tensile properties, and the material's J-R curve. Also inputted are loads, required safety margins on load, maximum allowable values of flaw depth and the J-integral, and the allowable values of ω, ρ and $\Delta a/b$ (see Section 3.3). Crack extension due to ductile tearing is modelled in equal increments DA. The applied primary load is increased at each increment to maintain equilibrium, as given by equation (3.1). The load at each increment is determined by Newton-Raphson iteration.

The ductile tearing continues until one of the following limiting conditions is reached:

a) The inputted maximum allowable flaw depth. The final load at this flaw depth is determined by Newton-Raphson iteration.

b) The inputted maximum allowable value of the J-integral. The load at this flaw depth is determined.

c) The limit of $\Delta a/b$ for J-controlled crack growth, where b is the remaining ligament (see Section 3.3). The load at this flaw depth is determined.

d) The inputted minimum value of ω for J-controlled crack growth. The load at this flaw depth is determined.

e) The inputted minimum allowable value of ρ for J-controlled crack growth. The load at this flaw depth is determined.

f) The primary load reaching: (initial primary load) x (required margin on primary load). The flaw depth at which the margin on primary load is equal to the required margin is determined by using Newton–Raphson iteration.

g) The flaw reaching instability. The stability/instability condition is given by equation (3.5). The flaw depth and load at instability are determined by solving equations (3.1) and (3.2) simultaneously. The solution technique is a Newton–Raphson iteration.

The program prints out which limiting condition was reached first.

Procedure 2 uses all of the basic subroutines of which Procedure 1 consists.

5.3 Procedure 3 – Finding Limiting Initial Flaw Depth

The user inputs the model dimensions, starting value of initial flaw size, material tensile properties, and the material's J–R curve. Also inputted are the loads, required safety margins on load, maximum allowable values of flaw depth and the J–integral, and the allowable values of ω, ρ, and $\Delta a/b$. The solution algorithm is given below.

i. Solve for the primary load at crack extension instability by using Newton–Raphson iteration.

ii. Check if any of the criteria a) to e) of Section 5.2 were exceeded.

iii. If any of the criteria a) to e) were exceeded, reduce the flaw depth to a value which meets the criteria. Determine the primary load by Newton–Raphson iteration.

iv. Check if the margin on primary load is less than the required margin. If so, estimate the flaw depth at which the margin on load is equal to the required margin by linear interpolation. Go to step i.

v. If the margin on load exceeds the required margin, increment the initial flaw depth by a fixed amount DAO and go to step i.

vi. If the margin on load is equal to the required margin within a tolerance, the solution has been reached.

The program prints out which limiting condition was reached first.

Procedure 3 uses essentially all of the subroutines used in Procedures 1 and 2.

6.0 VALIDATION

The validation exercise resulted in the validation of the computer coding only. The accuracy of the J–integral estimation formulae is implicitly assumed.

The computer program is modular in structure. The majority of the subroutines are independent of the particular flaw model. Thus, once these independent subroutines have been validated for the three current cracked cylinder models, the subroutines can be considered reliable for other flaw models.

The validation was performed in a step-wise fashion from Procedure 1 to Procedure 3, in which the lower-level subroutines were validated prior to the higher-level subroutines. The validation of Procedure 1 results in the validation of the calculation of the J-integral and tearing modulus. Procedure 2 involves the validation of the controller for modelling stable crack extension, and the Newton-Raphson iteration schemes including the partial derivatives of J and T required in the schemes. Procedure 3 involves the validation of the controller for finding the maximum allowable initial flaw depth. All three flaw models were employed in the validation of each procedure.

Validation of Procedure 1

The dimensions of the three flaw models are given in Table 6-1, the material properties in Table 6-2, and the applied loads in Table 6-3. The input data files are given in Appendix B of this report.

The J-integral and tearing modulus were calculated manually using the formulae. The tearing modulus was determined by forward finite-differencing J-integral values, such that the tearing modulus corresponds to a flaw of depth a_o + 0.025 mm. The tearing modulus calculated by the computer program also corresponds to a flaw depth a_o + 0.025 mm. The results from the computer program and hand calculation are compared in Table 6-4. Close agreement was reached.

The subroutines containing the functions F_p, F_m, F_b and h_1 (see equations 3.8 and 3.16) were driven independent of the main program to check the complete range of values against the documented values.

Validation of Procedure 2

The dimensions of the three flaw models are given in Table 6-1, the material properties in Table 6-2, and the initial applied loads in Table 6-5. Seven runs were performed to test each of the limiting criteria given in Section 5.2. The controlling parameters for each run are given in Tables 6-6, 6-8 and 6-10 for Models 1, 2 and 3, respectively. One sample input file for each model, for Run 7, is given in Appendix B. The computer program printout includes both the applied and the material's resistance values of the J-integral and tearing modulus. This allows the user to check that both crack equilibrium (equation (3.1)) and crack stability (equation (3.5)) are satisfied prior to the point of crack instability.

The results are summarized in Tables 6-7, 6-9 and 6-11 for Models 1, 2, and 3, respectively. The run which displayed the maximum amount of crack extension was Run 7, in which the cracked structure was loaded up to instability. The appropriate limiting criteria were satisfied in all seven runs.

Validation of Procedure 3

For a given initial flaw depth a_0, the cracked structure was loaded up by increasing the primary load until the stable crack extension reached some limit, such as an inputted maximum value of the J-integral, or instability. This procedure was repeated for increasing values of a_0 until the margin on primary load at the limiting state was reduced to 2.77. Seven runs were performed. The input parameters for each run were modified such that a different criterion in Section 5.3 limited crack extension in each run.

The dimensions of the three flaw models are given in Table 6-1, the material properties are given in Table 6-2, and the initial applied loads are given in Table 6-12. The inputted controlling parameters for each run are given in Tables 6-13, 6-15 and 6-17 for Models 1, 2 and 3, respectively. One sample input file for each flaw model, for Run 7, is given in Appendix B. The computer program printout includes both the applied and the material's resistance values of the J-integral and tearing modulus to allow the user to check that both crack equilibrium and crack stability are satisfied prior to the point of instability.

The results are summarized in Tables 6-14, 6-16 and 6-18 for Models, 1, 2 and 3, respectively. The appropriate limiting criteria were satisfied in all seven runs.

Reviewed:

B. Mukherjee
Acting Section Head
Nondestructive and Fracture
Evaluation Section

Prepared:

D.A. Scarth
Engineer
Nondestructive and Fracture
Evaluation Section

Approved:

J. Brown
Manager
Metallurgical Research Dept

DAS:SEHG

REFERENCES

1. Draft IWB-3650, "Acceptance Criteria for Flaws in Ferritic Piping", and Appendix Z, "Evaluation of Flaws in Ferritic Piping", prepared by the ASME Section XI Task Group on Pipe Flaw Evaluation, January, 1988.

2. Bloom, J.M., "User's Guide for the Failure Assessment Diagram – Computer Code FAD", Revision 3a, Babcock and Wilcox, Alliance, Ohio, October, 1987.

3. Kumar, V., German, M.D. and Shih, C.F., "An Engineering Approach for Elastic-Plastic Fracture Analysis", EPRI Report No. NP-1931, Research Project No. 1237-1, General Electric Co., July, 1981.

4. Bloom, J.M. and Malik, S.M., "Procedure for the Assessment of the Integrity of Nuclear Pressure Vessels and Piping Containing Defects", EPRI Report NP-2431, Research Project 1237-2, Babcock and Wilcox Co., June, 1982.

5. Rice, J.R., "A Path Independent Integral and the Approximate Analysis of Strain Concentration by Notches and Cracks", Journal of Applied Mechanics, pp 379-386, June, 1968.

6. Scarth, D.A., "Development of a Computer Program for Performing Engineering Approach Elastic-Plastic Fracture Mechanics Flaw Evaluations", Metallurgical Research Department, Report no. 86-246-K, File No. 826.222, November 11, 1986.

7. Hutchinson, J.W. and Paris, P.C., "Stability Analysis of J-Controlled Crack Growth", Elastic-Plastic Fracture, ASTM STP 668, pp 37-64, 1979.

8. Mendelson, A., "Plasticity: Theory and Application", The MacMillan Co., 1968.

9. Kumar, V., et al, "Advances in Elastic-Plastic Fracture Analysis", EPRI Report No. NP-3607, Research Project 1237-1, General Electric Co., August, 1984.

10. "Standard Test Method for Determining J-R Curves", ASTM Standard E1152, ASTM Annual Book of Standards, 1987, Vol. 03.01, pp 1129-1145.

11. Tada, H., Paris, P.C. and Irwin, G.R., "The Stress Analysis of Cracks Handbook, "Del Research Corporation, St. Louis, Missouri, 1973.

12. Buchalet, C.B. and Bamford, W.H., "Stress Intensity Factor Solutions for Continuous Surface Flaws in Reactor Pressure Vessels", ASTM STP 590, pp 385-402, 1976.

13. Raju, I.S. and Newman, J.C., "Stress-Intensity Factors for Internal and External Surface Cracks in Cylindrical Pressure Vessels", ASME Journal of Pressure Vessel Technology, Vol. 104, pp 293-298, November, 1982.

14. Wilkening, W.W., deLorenzi, H.G. and Barishpolsky, M., "Elastic-Plastic Analysis of Surface Flaws in a Reactor Vessel", ASME Journal of Pressure Vessel Technology, Vol, 106, pp 247-254, August, 1984.

15. Bloom, J.M., "Extensions of the Failure Assessment Diagram Approach: Semi-Elliptical Flaw in Pressurized Cylinders – Part II", ASME Journal of Pressure Vessel Technology, Vol. 108, pp 485-489, November 1986.

16. "ABAQUS-User's Manual", Version 4.6-161, Hibbitt, Karlsson and Sorensen, Inc., Providence, Rhode Island, 1986.

17. Scarth, D.A., "Final Progress Report for 1986 on the Development of Elastic-Plastic Fracture Mechanics Methodologies", Metallurgical Research Department, Report No. M86-150-K, File No. 826.222, January 6, 1987.

TABLE 6-1

Dimensions of Models Used in the Validation Cases

Dimension	Model 1 - 360° Circumferential Flaw	Model 2 - Infinitely Long Axial Flaw	Model 3 - Semi-Elliptical Axial Flaw
Inner Radius, R_i (mm)	810	275.8	275.8
Wall Thickness, t (mm)	72	29	29
Initial Flaw Depth, a_o (mm)	9	8.7*	8.7**
a_o/t	0.125	0.300*	0.300**
a/c	0.0	0.0	0.333

*In Procedure 3, a = 4.35 mm.
**In Procedure 3, a = 5.80 mm.

TABLE 6-2

Material Properties for Validation Cases

Property	Model 1 - 360° Circumferential Flaw	Model 2 - Infinitely Long Axial Flaw	Model 3 - Semi-Elliptical Axial Flaw
Young's Modulus, E (MPa)	209×10^3	200×10^3	200×10^3
Poisson's Ratio, ν	0.3	0.3	0.3
Yield Stress, σ_o (MPa)	255	275	275
Flow Stress, σ_f (MPa)	350	362	362
Ramberg-Osgood Constants: α	2.81	2.2	2.2
n	4.88	8.0	8.0
J-R Curve Representation:			
C_1 (N/m)	1.6319×10^6	1.4927×10^6	1.4927×10^6
C_2 (for a in m)	0.3442	0.3527	0.3527

TABLE 6-3

Applied Loads Used in the Validation of Procedure 1

Load	Model 1 - 360° Circumferential Flaw	Model 2 - Infinitely Long Axial Flaw	Model 3 - Semi-Elliptical Axial Flaw
Primary Load	remote stress = 284.91 MPa	internal pressure = 29.685 MPa	internal pressure = 29.685 MPa
Secondary Membrane Stress (MPa)	25.90	20.00	20.00
Secondary Pure Through-Wall Bending Stress (MPa)	30.00	70.00	70.00

TABLE 8-4

Results from Validation of Procedure 1

Case	J-Integral (kN/m)		Tearing Modulus	
	Hand Calculation	Computer Program	Hand Calculation	Computer Program
Model 1	114.88	114.88	32.975	32.996
Model 2	476.49	476.49	314.24	313.84
Model 3	70.267	70.265	20.813	20.825

TABLE 6-5

Applied Loads Used in the Validation of Procedure 2

Load	Model 1 - 360° Circumferential Flaw	Model 2 - Infinitely Long Axial Flaw	Model 3 - Semi-Elliptical Axial Flaw
Primary Load	remote stress = 167.00 MPa	internal pressure = 15.00 MPa	internal pressure = 15.00 MPa
Secondary Membrane Stress (MPa)	30.00	10.00	10.00
Secondary Pure Through-Wall Bending Stress (MPa)	40.00	60.00	60.00

TABLE 6-8

Inputted Controlling Parameters for
Validation of Procedure 2 Using Model 1

Run	Maximum Allowable Final Crack Depth, a_{max} (mm)	Maximum Allowable J-Integral, J_{max} (kN/m)	Required Margin on Primary Load	Maximum Allowable $\Delta a/b$	Minimum Allowable ω	Minimum Allowable ρ
1 - Limit on a_{max}	10.5	54×10^6	2.770	0.06	10.0	25.0
2 - Limit on J_{max}	70	180	2.770	0.06	10.0	25.0
3 - Limit on Load	54	54×10^6	1.7211	0.06	10.0	25.0
4 - Limit on $\Delta a/b$	54	54×10^6	2.770	0.03	5.0	25.0
5 - Limit on ω	54	54×10^6	2.770	0.06	20.0	25.0
6 - Limit on ρ	54	54×10^6	2.770	0.06	10.0	80.0
7 - Limit on Instability	54	54×10^6	2.770	0.06	5.0	25.0

TABLE 8-7

Results of Validation of Procedure 2 Using Model 1

Run	Final Crack Depth, a (mm)	Final Margin on Primary Load	Final J (kN/m)	Final T_R	Final T_J	Final $\Delta a/b$	Final ω	Final ρ
1 - Limit on a_{max}	10.50	1.760	174.1	68.15	45.70	0.02439	14.11	80.08
2 - Limit on J_{max}	10.65	1.763	180.0	63.95	46.91	0.02694	12.78	86.91
3 - Limit on Load	9.78	1.721	138.8	105.01	37.75	0.01247	27.60	114.35
4 - Limit on $\Delta a/b$	10.83	1.766	186.6	59.71	48.21	0.03000	11.47	83.59
5 - Limit on ω	10.07	1.743	154.8	85.27	41.51	0.01721	20.00	102.04
6 - Limit on ρ	11.03	1.768	194.2	55.32	49.66	0.03384	10.17	80.00
7 - Limit on Instability	11.32	1.769	202.4	51.14	51.14	0.03831	8.98	76.44

TABLE 6-8

Inputted Controlling Parameters for
Validation of Procedure 2 Using Model 2

Run	Maximum Allowable Final Crack Depth, a_{max} (mm)	Maximum Allowable J-Integral, J_{max} (kN/m)	Required Margin on Primary Load	Maximum Allowable $\Delta a/b$	Minimum Allowable ω	Minimum Allowable ρ
1 - Limit on a_{max}	9.5	81×10^6	2.770	0.08	5.0	25.0
2 - Limit on J_{max}	21.75	125	2.770	0.08	5.0	25.0
3 - Limit on Load	21.75	81×10^6	1.520	0.08	5.0	25.0
4 - Limit on $\Delta a/b$	21.75	81×10^6	2.770	0.04	5.0	25.0
5 - Limit on ω	21.75	81×10^6	2.770	0.08	10.0	25.0
6 - Limit on ρ	21.75	81×10^6	2.770	0.08	5.0	45.0
7 - Limit on Instability	21.75	81×10^6	2.770	0.08	5.0	25.0

TABLE 8-9

Results of Validation of Procedure 2 Using Model 2

Run	Final Crack Depth, a (mm)	Final Margin on Primary Load	Final J (kN/m)	Final T_R	Final T_J	Final $\Delta a/b$	Final ω	Final ρ
1 - Limit on a_{max}	9.50	1.547	120.7	81.21	67.83	0.04103	8.60	44.43
2 - Limit on J_{max}	9.58	1.548	125.0	76.15	70.21	0.04551	7.75	42.72
3 - Limit on Load	9.10	1.520	94.9	126.23	52.96	0.02034	17.34	57.65
4 - Limit on $\Delta a/b$	9.48	1.547	119.7	82.50	67.25	0.04000	8.82	44.86
5 - Limit on ω	9.39	1.544	114.7	89.24	64.43	0.03527	10.00	47.03
6 - Limit on ρ	9.47	1.547	119.3	82.94	67.06	0.03968	8.89	45.00
7 - Limit on Instability	9.66	1.549	128.7	72.22	72.22	0.04958	7.11	41.34

TABLE 6-10

Inputted Controlling Parameters for
Validation of Procedure 2 Using Model 3

Run	Maximum Allowable Final Crack Depth, a_{max} (mm)	Maximum Allowable J-Integral, J_{max} (kN/m)	Required Margin on Primary Load	Maximum Allowable $\Delta a/b$	Minimum Allowable ω	Minimum Allowable ρ
1 - Limit on a_{max}	9.5	81×10^6	2.770	0.06	5.0	25.0
2 - Limit on J_{max}	21.75	125	2.770	0.06	5.0	25.0
3 - Limit on Load	21.75	81×10^6	2.100	0.06	5.0	25.0
4 - Limit on $\Delta a/b$	21.75	81×10^6	2.770	0.04	5.0	25.0
5 - Limit on ω	21.75	81×10^6	2.770	0.06	10.0	25.0
6 - Limit on ρ	21.75	81×10^6	2.770	0.06	5.0	45.0
7 - Limit on Instability	21.75	81×10^6	2.770	0.10	4.0	25.0

TABLE 6-11

Results of Validation of Procedure 2 Using Model 3

Run	Final Crack Depth, a (mm)	Final Margin on Primary Load	Final J (kN/m)	Final T_R	Final T_J	Final $\Delta a/b$	Final ω	Final ρ
1 - Limit on a_{max}	9.50	2.095	120.7	81.21	40.23	0.04103	8.60	44.43
2 - Limit on J_{max}	9.58	2.099	125.0	78.15	42.06	0.04551	7.75	42.72
3 - Limit on Load	9.58	2.100	125.5	75.57	42.29	0.04607	7.65	42.51
4 - Limit on $\Delta a/b$	9.46	2.094	118.7	82.50	39.80	0.04000	8.82	44.86
5 - Limit on ω	9.39	2.087	114.7	89.24	37.74	0.03527	10.00	47.03
6 - Limit on ρ	9.47	2.093	118.3	82.94	39.66	0.03966	8.89	45.00
7 - Limit on Instability	10.20	2.112	150.7	54.05	54.05	0.07981	4.42	34.31

TABLE 6-12

Applied Loads Used in the Validation of Procedure 3

Load	Model 1 - 360° Circumferential Flaw	Model 2 - Infinitely Long Axial Flaw	Model 3 - Semi-Elliptical Axial Flaw
Primary Load	remote stress = 100.00 MPa	internal pressure = 10.00 MPa	internal pressure = 10.00 MPa
Secondary Membrane Stress (MPa)	30.00	10.00	10.00
Secondary Pure Through-Wall Bending Stress (MPa)	40.00	60.00	60.00

TABLE 8-13

Inputted Controlling Parameters for
Validation of Procedure 3 Using Model 1

Run	Maximum Allowable Initial Crack Depth a_{omax} (mm)	Maximum Allowable Final Crack Depth, a_{max} (mm)	Maximum Allowable J-Integral J_{max} (kN/m)	Maximum Allowable $\Delta a/b$	Minimum Allowable ω	Minimum Allowable ρ
1 - Limit on a_{omax}	11	54	54×10^6	0.08	5.0	25.0
2 - Limit on a_{max}	13	13	54×10^6	0.08	5.0	25.0
3 - Limit on J_{max}	54	54	200	0.08	5.0	25.0
4 - Limit on $\Delta a/b$	54	54	54×10^6	0.03	5.0	25.0
5 - Limit on ω	54	54	54×10^6	0.08	10.0	25.0
6 - Limit on ρ	54	54	54×10^6	0.08	5.0	75.0
7 - Limit on Instability	54	54	54×10^6	0.08	5.0	25.0

Initial crack depth = 9 mm.

TABLE 6-14

Results of Validation of Procedure 3 Using Model 1

Run	Final Value of a_o (mm)	Final Crack Depth (mm)	Margin on Load at Final Value of a_o	Final J (kN/m)	Final T_R, T_J	Final $\Delta a/b$	Final ω	Final ρ
1 - Limit on a_{omax}	11.00	13.55	2.795	209.0	46.12, 46.12	0.04363	7.89	71.32
2 - Limit on a_{max}	11.21	13.00	2.770	185.2	60.59, 43.31	0.03042	11.31	81.24
3 - Limit on J_{max}	11.32	13.57	2.770	200.0	52.32, 45.94	0.03841	8.96	74.50
4 - Limit on $\Delta a/b$	11.20	12.97	2.770	184.3	61.12, 43.16	0.03000	11.47	81.66
5 - Limit on ω	11.28	13.30	2.770	192.9	56.06, 44.67	0.03442	10.00	77.61
6 - Limit on ρ	11.32	13.52	2.770	198.8	52.91, 45.73	0.03773	9.12	75.00
7 - Limit on Instability	11.34	13.83	2.770	209.9	47.71, 47.71	0.04449	7.74	70.54

TABLE 6-15

Inputted Controlling Parameters for
Validation of Procedure 3 Using Model 2

Run	Maximum Allowable Initial Crack Depth a_{omax} (mm)	Maximum Allowable Final Crack Depth, a_{max} (mm)	Maximum Allowable J-Integral J_{max} (kN/m)	Maximum Allowable $\Delta a/b$	Minimum Allowable ω	Minimum Allowable ρ
1 - Limit on a_{omax}	5.8	21.75	81 x 10^6	0.06	5.0	25.0
2 - Limit on a_{max}	6.5	6.5	81 x 10^6	0.06	5.0	25.0
3 - Limit on J_{max}	21.75	21.75	120	0.06	5.0	25.0
4 - Limit on $\Delta a/b$	21.75	21.75	81 x 10^6	0.035	5.0	25.0
5 - Limit on ω	21.75	21.75	81 x 10^6	0.06	10.0	25.0
6 - Limit on ρ	21.75	21.75	81 x 10^6	0.06	5.0	55.0
7 - Limit on Instability	21.75	21.75	81 x 10^6	0.06	5.0	25.0

Initial crack depth = 4.35 mm.

TABLE 8-18

Results of Validation of Procedure 3 Using Model 2

Run	Final Value of a_o (mm)	Final Crack Depth (mm)	Margin on Load at Final Value of a_o	Final J (kN/m)	Final T_R, T_J	Final $\Delta a/b$	Final ω	Final ρ
1 - Limit on a_{omax}	5.90	6.72	2.778	121.8	79.62, 79.62	0.03688	9.56	50.29
2 - Limit on a_{max}	5.91	6.50	2.770	108.5	98.67, 71.63	0.02832	13.40	57.00
3 - Limit on J_{max}	5.95	6.73	2.770	120.0	82.08, 78.48	0.03534	9.98	51.03
4 - Limit on $\Delta a/b$	5.95	6.73	2.770	119.8	82.58, 78.24	0.03500	10.08	51.22
5 - Limit on ω	5.95	6.73	2.770	119.9	82.19, 78.43	0.03527	10.00	51.07
6 - Limit on ρ	5.93	6.58	2.770	112.1	92.97, 73.77	0.02885	12.18	55.00
7 - Limit on Instability	5.95	6.77	2.770	122.0	79.66, 79.66	0.03708	9.51	50.12

TABLE 6-17

Inputted Controlling Parameters for
Validation of Procedure 3 Using Model 3

Run	Maximum Allowable Initial Crack Depth a_{omax} (mm)	Maximum Allowable Final Crack Depth, a_{max} (mm)	Maximum Allowable J-Integral J_{max} (kN/m)	Maximum Allowable $\Delta a/b$	Minimum Allowable ω	Minimum Allowable ρ
1 - Limit on a_{omax}	12	21.75	81 x 10^6	0.06	5.0	25.0
2 - Limit on a_{max}	11.6	11.6	81 x 10^6	0.10	4.0	25.0
3 - Limit on J_{max}	21.75	21.75	120	0.10	4.0	25.0
4 - Limit on $\Delta a/b$	21.75	21.75	81 x 10^6	0.04	4.0	25.0
5 - Limit on ω	21.75	21.75	81 x 10^6	0.06	10.0	25.0
6 - Limit on ρ	21.75	21.75	81 x 10^6	0.06	5.0	40.0
7 - Limit on Instability	21.75	21.75	81 x 10^6	0.10	4.0	25.0

Initial crack depth = 5.8 mm.

TABLE 6-18

Results of Validation of Procedure 3 Using Model 3

Run	Final Value of a_o (mm)	Final Crack Depth (mm)	Margin on Load at Final Value of a_o	Final J (kN/m)	Final T_R, T_J	Final $\Delta a/b$	Final ω	Final ρ
1 - Limit on a_{omax}	12.00	12.96	2.818	128.8	72.06, 56.00	0.06000	5.88	34.24
2 - Limit on a_{max}	11.35	11.60	2.770	80.12	172.27, 29.12	0.01439	24.51	59.72
3 - Limit on J_{max}	12.36	13.15	2.770	120.0	82.08, 52.31	0.04985	7.10	36.32
4 - Limit on $\Delta a/b$	12.26	12.90	2.770	111.8	93.45, 47.24	0.04000	8.82	39.60
5 - Limit on ω	12.18	12.75	2.770	107.3	100.78, 44.51	0.03527	10.00	41.65
6 - Limit on ρ	12.24	12.87	2.770	110.9	94.86, 46.88	0.03901	9.04	40.00
7 - Limit on Instability	12.45	13.61	2.770	137.4	64.02, 64.02	0.07506	4.70	30.81

APPENDIX A

Formulation of the Fully-Plastic h_1 Function for Semi-Elliptical Axial Flaws

Elastic-plastic J-integral solutions for t/R_i = 0.10, n = 8.6, a/c = 0.333 and a/t = 0.25 to 0.75 are given by Wilkening et al in /14/. Fully-plastic h_1 functions were determined from these solutions by Bloom/15/ by using a curve fitting procedure with the Deformation Plasticity Failure Assessment Diagram approach. The h_1 functions are plotted on log-linear scales in Figure A-1.

The value of the h_1 functions were also checked by the author of this report. The fully-plastic J-integral was first calculated from the solutions in /14/ by using

$$J_p(a) = J_{ep}(a_e) - J_e(a_e) \qquad (A.1)$$

where $J_{ep}(a_e)$ is taken from /14/. The value of h_1 was then calculated from $J_p(a)$ by inverting equation (3.16) in Section 3.2. The resulting h_1 functions were found to be in reasonable agreement with those given in /15/.

Values of h for a/t = 0.25 to 0.75 and for n = 7.0 and n = 10.0 were estimated as suggested in /15/ by prorating the values for n = 8.6 based on the h_1 values for the two-dimensional infinitely long axial flaw given in /3/.

$$h_1(3D,\ n{=}n_i) = \frac{h_1(2D,\ n{=}n_i)}{h_1(2D,\ n{=}8.6)}\ h_1(3D,\ n{=}8.6) \qquad (A.2)$$

The two-dimensional h_1 values are given in Table 4-9 of this report. The two-dimensional h_1 values are relatively insensitive to n in this range.

The values of the h_1 function for a/t = 0.125, a/c = 0.333, t/R_i = 0.10 at n = 7.0 and 8.6 were determined from in-house finite-element calculations performed by running the computer program ABAQUS/16/. The calculations were performed for a semi-elliptical circumferential flaw rather than an axial flaw. A similar calculation is described in /17/. The J-integral at this shallow flaw depth is considered to be insensitive to cylinder geometry for this high value of R_i/t (= 10), provided the appropriate stress field is applied.

The hoop stress in the pressurized cylinder has a pure membrane component of magnitude $p \cdot R_i/t$, plus a pure through-wall bending component of magnitude $+0.06 \cdot p\ R_i/t$ at the inside wall. The internal pressure p is also acting on the crack faces. The applied pure membrane stress acting on the circumferentially cracked cylinder in the finite-element calculations had a magnitude of $p\ R_i/t$, with no bending component. The pressure acting on the crack faces in the model had a magnitude of $0.20 \cdot p \cdot R_i/t$, which would conservatively account for both the pressurization of the crack faces and the through-wall bending stress in the axial flaw case.

The h_1 functions for a/t = 0.125 were calculated by using equation (A-1) and (3.16) in Section 3.2. As described earlier, the h_1 function value for n = 10.0 was estimated by prorating the n = 8.6 result by using equation (A-2). The h_1 value for a/t = 0.125 and n = 8.6 is also plotted on Figure A-1.

Linear interpolation of the h_1 function on the log-linear scales between the data points resulted in numerical inconsistencies when calculating the derivative dJ/da. The variation of h_1 with a/t was conservatively idealized by the straight line drawn on Figure A-1. The degree of conservatism only becomes significant for a/t greater than 0.45. This straight line fit eliminated the numerical inconsistencies, and was adopted for all three values of n. The final values of h_1 are given in Table 4-12. Linear interpolation on the log-linear scales is used between data points when interpolating over a/t. Linear interpolation on linear scales is used to interpolate over n.

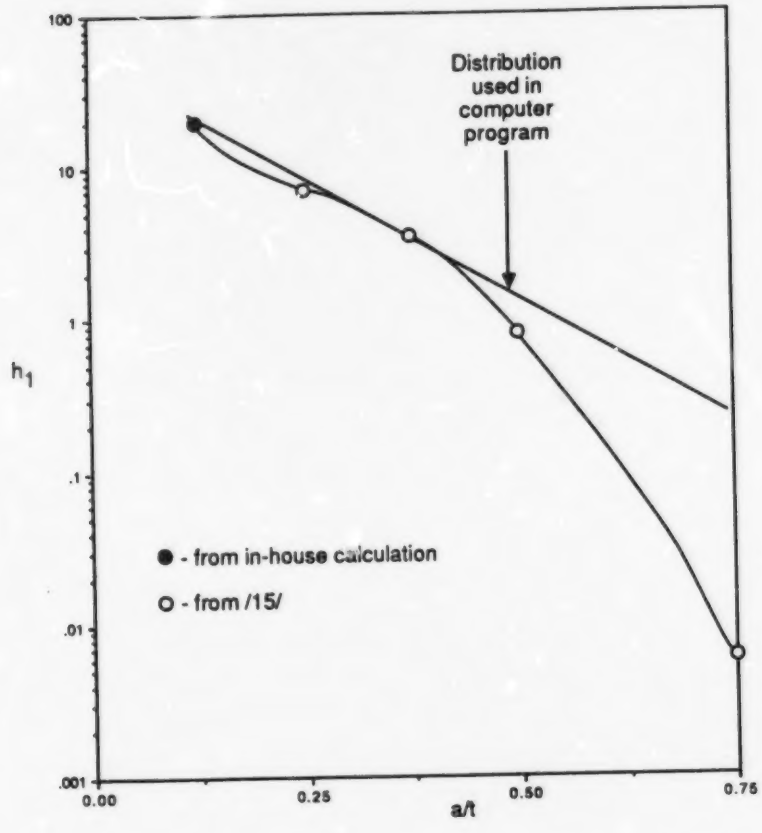

FIGURE A-1
VARIATION OF h_1 FUNCTION WITH a/t
FOR SEMI-ELLIPTICAL AXIAL CRACK, WITH a/c = 0.333,
t/R_i = 0.10 AND n = 8.6

APPENDIX B

Input Description

Any consistent set of units may be used. It is recommended that only the basic values of a set of units be used (eg. Pa instead of MPa) to reduce the possibility of errors. The validity limits of each flaw model are given in Table 4–1.

The word "INPUT>" given below precedes the data to be input on a line. Input is format free and should be terminated with a "/". If an item is not entered it will either be set to a default value if given below, or will be assigned a value of zero.

Input data must be entered as an input file named in the format of: filename.INP. An outfile named: filename.LIS will be generated.

B1 Input for Procedure 1

B1.1 Title

INPUT> title of run.

Maximum of 80 characters, not enclosed in quotes.

B1.2 Procedure and Model Type

INPUT> 'JT-GENERATE', 'model type'

Enclose words in quotes. The currently available model types are:

CYL-INT-360-CIRCUM-EDGE-TENSION
CYL-INT-LONG-AXIAL-EDGE-PRESS
CYL-INT-ELLIP-AXIAL-EDGE-PRESS

Defaults: none.

B1.3 Dimensions

For Model Type = CYL-INT-360-CIRCUM-EDGE-TENSION or
CYL-INT-LONG-AXIAL-EDGE-PRESS

INPUT> inner radius, outer radius.

INPUT> NUMGEN (= number of cases)

Repeat NUMGEN times:

INPUT> (crack depth)/(wall thickness)

For Model Type = CYL-INT-ELLIP-AXIAL-EDGE-PRESS

INPUT> inner radius, outer radius

INPUT> NUMGEN (= number of cases)

Repeat NUMGEN times:

INPUT> (crack depth)/(wall thickness),
(crack depth)/(half crack length)

Defaults: none.

B1.4 Material Properties

Tensile Properties:

INPUT> Young's Modulus, Poisson's ratio

INPUT> yield stress, flow stress, Ramberg-Osgood constant α, Ramberg-Osgood constant n

Defaults: none.

B1.5 Load Cases

For Model Type = CYL-INT-360-CIRCUM-EDGE-TENSION:

Repeat NUMGEN times:

INPUT> applied primary membrane stress,
applied secondary membrane stress,
applied secondary pure through-wall bending stress.

For Model type = CYL-INT-LONG-AXIAL-EDGE-PRESS
or CYL-INT-ELLIP-AXIAL-EDGE-PRESS

Repeat NUMGEN times:

INPUT> internal pressure,
applied secondary membrane stress,
applied secondary pure through-wall bending stress.

Defaults: none.

B1.6 Sample Input

The input files for the three validation cases for Procedure 1 are given below.

TEST CASE 1 - TO CHECK JT-GENERATE OPTION FOR EPFLAW DEVELOPMENT

```
'JT-GENERATE', 'CYL-INT-360-CIRCUM-EDGE-TENSION'/
0.810, 0.882 / RI, RO

2 / NUMSET
0.1250000 / AOBSET
0.1256944 / AOBSET

2.09E11, 0.3/ E, V
255.0E6, 350.0E6, 2.81, 4.88/SIGO, SIGF, ALPHA, N

284.9141E6, 25.90128E6, 30.00E6 / PSET(IM), SIG2ND(IM), SIG2ND(IB)
284.9141E6, 25.90128E6, 30.00E6 / PSET(IM), SIG2ND(IM), SIG2ND(IB)
```

TEST CASE 2 - TO CHECK JT-GENERATE OPTION FOR EPFLAW DEVELOPMENT

```
'JT-GENERATE', 'CYL-INT-LONG-AXIAL-EDGE-PRESS'/

0.2758, 0.3048 / RI, RO

2 / NUMSET
0.3000000 / AOBSET
0.3017241 / AOBSET

2.00E11, 0.3/E, V
275.0E6, 362.0E6, 2.20, 8.00/SIGO, SIGF, ALPHA, N

29.68499E6, 20.0000E6, 70.0000E6 / PSET(IM), SIG2ND(IM), SIG2ND(IB)
29.68499E6, 20.0000E6, 70.0000E6 / PSET(IM), SIG2ND(IM), SIG2ND(IB)
```

TEST CASE 3 - TO CHECK JT-GENERATE OPTION FOR EPFLAW DEVELOPMENT

'JT-GENERATE', 'CYL-INT-ELLIP-AXIAL-EDGE-PRESS'/

0.2758, 0.3048 / RI, RO

2 / NUMSET
0.3000000, 0.3333333 / AOBSET, AOCSET
0.3017241, 0.3333333 / AOBSET, AOCSET

2.00E11, 0.3/E, V
275.0E6, 362.0E6, 2.20, 8.00/SIGO, SIGF, ALPHA, N

29.68499E6, 20.0000E6, 70.0000E6 / PSET(IM), SIG2ND(IM), SIG2ND(IB)
29.68499E6, 20.0000E6, 70.0000E6 / PSET(IM), SIG2ND(IM), SIG2ND(IB)

B2 Input for Procedure 2

B2.1 Title

Input described in Section B1.1

B2.2 Procedure and Model Type

INPUT> 'JT-FOLLOW-JR-CURVE', 'model type'

Enclose words in quotes. The currently available model types are:

CYL-INT-360-CIRCUM-EDGE-TENSION
CYL-INT-LONG-AXIAL-EDGE-PRESS
CYL-INT-ELLIP-AXIAL-EDGE-PRESS

Defaults: none.

B2.3 Dimensions

For Model Type = CYL-INT-360-CIRCUM-EDGE-TENSION
or CYL-INT-LONG-AXIAL-EDGE-PRESS

INPUT> inner radius, outer radius

INPUT> (crack depth)/(wall thickness)

For Model Type = CYL-INT-ELLIP-AXIAL-EDGE-PRESS

INPUT> inner radius, outer radius

INPUT> (crack depth)/(wall thickness),
(crack depth)/(half crack length)

B2.4 Material Properties

Tensile Properties:

INPUT> Young's Modulus, Poisson's ratio

INPUT> yield stress, flow stress, Ramberg-Osgood constant α, Ramberg-Osgood constant n

Defaults: none

Fracture Properties:

The J-R curve is idealized as:

$$J_R(\Delta a) = C_1 \ (\Delta a)^{C_2} \qquad \text{(B1)}$$

where the units are:

J_R - force/length,
Δa - length.

The component dimensions, J_R and Δa must be expressed in the same length unit. For example, if the J-R curve was correlated using units of N/m for J_R and mm for Δa, then C_1 must first be modified by

$$C_{1_{input}} = 1000^{C_2} \cdot C_{1_{correlated}} \qquad \text{(B2)}$$

Also, J_R must be expressed in the same force unit as Young's modulus and stresses.

INPUT> J-integral at crack initiation (= J_{Ic}), C_1, C_2

Defaults: none.

B2.5 Applied Loads

For Model Type = CYL-INT-360-CIRCUM-EDGE-TENSION

INPUT> applied primary membrane stress,
applied secondary membrane stress,
applied secondary pure through-wall bending stress.

For Model Type = CYL-INT-LONG-AXIAL-EDGE PRESS
or CYL-INT-ELLIP-AXIAL-EDGE-PRESS

INPUT> internal pressure,
applied secondary membrane stress,
applied secondary pure through-wall bending stress.

B2.6 Solution Control Parameters

INPUT> DA, AMAX, JMAX, SFPP, SFP2D

where

DA - crack extension increment, default = 0.075 x wall thickness

AMAX - maximum allowed flaw depth, default = 0.75 x wall thickness

JMAX - maximum allowed J-integral, default = $10^6 \cdot J_{Ic}$

SFPP - required safety margin on primary load to be reached, default = 2.77

SFP2D - required safety margin on secondary stress to be reached, default = 1.00

INPUT> maximum allowable $\Delta a/b$, minimum allowable ω, minimum allowable ρ.

Defaults: $\Delta a/b = 0.06$, $\omega = 10.0$, $\rho = 25.0$

Parameters to ensure J-controlled crack growth. See Section 3.3.

B2.7 Sample Input

The input files for validation case - Run 7 (limit = instability) for each of the three models for Procedure 2 are given below.

```
TEST RUN 7 - FOR JR-CURVE OPTION FOR EPFLAW DEVELOPMENT

'JT-FOLLOW-JR-CURVE', 'CYL-INT-360-CIRCUM-EDGE-TENSION'/

0.810, 0.882 / RI, RO
0.125 / AOBO
2.09E11, 0.3/E, V
255.0E6, 350.0E6, 2.81, 4.88 / SIGO, SIGF, ALPHA, N
54.0E3, 1.631927E6, 0.3441750 / JIC, CR, CP

167.00E6, 30.00E6, 40.00E6 / PAPPI(IM), SG2NDI(IM), SG2NDI(IB)

0.001, / DAI, AMAXI, XJMAXI, SFPPI, SFP2DI
 , 5.0 / GAMMAI, OMEGAI, RHOI
```

```
TEST RUN 7 FOR JR-CURVE OPTION FOR EPFLAW DEVELOPMENT

'JT-FOLLOW-JR-CURVE', 'CYL-INT-LONG-AXIAL-EDGE-PRESS'/

0.2758, 0.3048 / RI, RO
0.30000 / AOBO

2.00E11, 0.3/E, V
275.0E6, 362.0E6, 2.20, 8.00/ SIGO, SIGF, ALPHA, N
81.0E3, 1.4927E6, 0.3527 / JIC, CR, CP

15.0000E6, 10.0000E6, 60.0000E6 / PAPPI(IM), SG2NDI(IM), SG2NDI(IB)

0.0005, /DAI, AMAXI, XJMAXI, SFPPI, SFP2DI
 , 5.0 / GAMMAI, OMEGAI, RHOI


TEST RUN 7 FOR JR-CURVE OPTION FOR EPFLAW DEVELOPMENT

'JT-FOLLOW-JR-CURVE', 'CYL-INT-ELLIP-AXIAL-EDGE-PRESS'/

0.2758, 0.3048 / RI, RO
0.30000, 0.3333333 / AOBO, AOC
2.00E11, 0.3/E, V
275.0E6, 362.0E6, 2.20, 8.00/ SIGO, SIGF, ALPHA, N
81.0E3, 1.4927E6, 0.3527 / JIC, CR, CP

15.0000E6, 10.0000E6, 60.0000E6 / PAPPI(IM), SG2NDI(IM), SG2NDI(IB)

0.0005, /DAI, AMAXI, XJMAXI, SFPPI, SFP2DI
   0.10, 4.0 / GAMMAI, OMEGAI, RHOI
```

B3 Input for Procedure 3

B3.1 Title

Input described in Section B1.1.

B3.2 Procedure and Model Type

INPUT> 'CRIT-AO','model type'

Enclose words in quotes. The currently available model types are:

CYL-INT-360-CIRCUM-EDGE-TENSION
CYL-INT-LONG-AXIAL-EDGE-PRESS
CYL-INT-ELLIP-AXIAL-EDGE-PRESS

Defaults: none.

B3.3 Dimensions

Input described in Section B2.3.

B3.4 Material Properties

Input described in Section B2.4.

B3.5 Applied Loads

Input described in Section B2.5.

B3.6 Solution Control Parameters

INPUT> AMAX, JMAX, SFPP, SFP2D

Parameters described in Section B2.6.

INPUT> DAO, AOMAX

DAO = increment in initial flaw depth,
default = 0.075 x wall thickness

AOMAX = maximum allowed initial flaw depth,
default = 0.75 x wall thickness

INPUT> maximum allowable $\Delta a/b$, minimum allowable ω, minimum allowable ρ

Parameters to ensure J-controlled crack growth. See Section 3.3.

Defaults: $\Delta a/b = 0.06$, $\omega = 10.0$, $\rho = 25.0$

B3.7 Sample Input

The input files for validation case – Run 7 (limit = instability) for each of the models for Procedure 3 are given below.

```
TEST RUN 7 - TO CHECK CRIT-AO OPTION FOR EPFLAW DEVELOPMENT

'CRIT-AO', 'CYL-INT-360-CIRCUM-EDGE-TENSION'/

0.810, 0.882 / RI, RO
0.125 / AOBO

2.09E11, 0.3/E, V
255.0E6, 350.0E6, 2.81, 4.88 / SIGO, SIGF, ALPHA, N
54.0E3, 1.631927E6, 0.3441750 / JIC, CR, CP

100.00E6, 30.00E6, 40.00E6 / PAPPI(IM), SG2NDI(IM), SG2NDI(IB)

 / AMAX, JMAX, SFPP, SFP2
0.001 / DAO, AOMAX
  , 5.0 / GAMMAI, OMEGAI, RHOI
```

```
TEST RUN 7 TO CHECK CRIT-AO OPTION FOR EPFLAW DEVELOPMENT

'CRIT-AO', 'CYL-INT-LONG-AXIAL-EDGE-PRESS'/

0.2758, 0.3048 / RI, RO
0.1500 / AOBO

2.00E11, 0.3/E, V
275.0E6, 362.0E6, 2.20, 8.00/ SIGO, SIGF, ALPHA, N
81.0E3, 1.4927E6, 0.3527 / JIC, CR, CP
10.0000E6, 10.0000E6, 60.0000E6 / PAPPI(IM), SG2NDI(IM), SG2NDI(IB)

 / AMAX, JMAX, SFPP, SFP2
0.0005, /DAO, AOMAX
 , 5.0 / GAMMAI, OMEGAI, RHOI


TEST RUN 7 TO CHECK CRIT-AO OPTION FOR EPFLAW DEVELOPMENT

'CRIT-AO', 'CYL-INT-ELLIP-AXIAL-EDGE-PRESS'/

0.2758, 0.3048 / RI, RO
0.20000, 0.3333333 / AOBO, AOC

2.00E11, 0.3/E, V
275.0E6, 362.0E6, 2.20, 8.00/ SIGO, SIGF, ALPHA, N
81.0E3, 1.4927E6, 0.3527 / JIC, CR, CP

10.0000E6, 10.0000E6, 60.0000E6 / PAPPI(IM), SG2NDI(IM), SG2NDI(IB)

 / AMAX, JMAX, SFPP, SFP2
0.0005, / DAO, AOMAX
0.10, 4.0 / GAMMAI, OMEGAI, RHOI
```